Photothermal Patterning of Microgel/Gold Nanoparticle Composite Colloidal Crystals

Clinton D. Jones and L. Andrew Lyon*

Contribution from the School of Chemistry and Biochemistry, Georgia Institute of Technology, Atlanta, Georgia 30332-0400

Received June 24, 2002; E-mail: lyon@chemistry.gatech.edu

Abstract: We present a new method for laser direct writing in self-assembled hydrogel microparticle colloidal crystals via photothermal excitation of co-assembled colloidal Au particles. Close-packed colloidal crystals are assembled from ~224 nm diameter, thermoresponsive, poly-*N*-isopropylacrylamide hydrogel micro-particles (microgels); these crystals display sharp Bragg diffraction peaks in the mid-visible region of the spectrum due to the periodic dielectric function of the assembly. Raising the temperature of the crystal above the characteristic volume phase transition temperature of the microgel particles results in a reversible melting of the crystalline material due to the particle-based deswelling event. This transition can be used either to anneal defects from the crystalline material or to controllably and reversibly convert the assembly from the colored, crystalline state to a nondiffracting glassy material. Crystal-to-glass transitions are similarly accomplished via photothermal excitation when 16 nm diameter colloidal Au particles are co-assembled with the responsive microgels. Excitation of the colloidal Au plasmon absorption with a frequency doubled Nd:YAG laser ($\lambda = 532$ nm) results in optically directed conversion of either glasses to crystals or crystals to glasses, depending on the initial state of the assembly and the illumination time. These results represent a fundamentally new method for the patterning of self-assembled photonic materials.

Introduction

The self-assembly of three-dimensional (3-D) colloidal crystals is a process of broad interest due to its applicability to many pursuits, such as studies of condensed matter phase behavior,[1-5] the fabrication of mesoporous films,[6-10] and the development of photonic materials.[11-16] The latter application takes advantage of the periodicity in the material dielectric function to manipulate the flow of light through strong diffraction effects. Such effects have been applied to the fabrication of chemical sensors,[17] optical waveguides,[18] and optical switches.[19,20] In the case of materials designed to diffract in the visible spectral region, colloidal crystals offer some advantages over structures prepared by photolithographic or micro-machining methods, which have serious limitations at length scales approaching the diffraction limit. Furthermore, the chemically directed assembly of colloidal crystals offers new opportunities for materials with unique photoemission proper-ties,[21] tunable/switchable crystals,[17,22] and photonic materials that can be patterned following assembly.[12] This contribution focuses on colloidal crystal patterning.

With respect to photonic device applications, 3-D periodic structures hold the promise of light confinement and manipula-tion with far greater efficiency than typical approaches based on refraction (e.g., prisms) and reflection (e.g., traditional fiber optics).[23] However, to guide light efficiently through a photonic structure, nonphotonic regions must be present in the form of point, line, or plane "defects". In this construct, the light is permitted to propagate through the defect, while the surrounding photonic material confines the radiation to that defect.[23-25] It

(1) Hiltner, P. A.; Krieger, I. M. *J. Phys. Chem.* **1969**, *73*, 2386.
(2) Dinsmore, A. D.; Crocker, J. C.; Yodh, A. G. *Curr. Opin. Colloid Interface Sci.* **1998**, *3*, 5−11.
(3) Pieranski, P. *Contemp. Phys.* **1983**, *24*, 25−73.
(4) Monovoukas, Y.; Gast, A. P. *Langmuir* **1991**, *7*, 460−468.
(5) Cheng, Z. D.; Zhu, J. X.; Russel, W. B.; Chaikin, P. M. *Phys. Rev. Lett.* **2000**, *85*, 1460−1463.
(6) Velev, O. D.; Kaler, E. W. *Adv. Mater.* **2000**, *12*, 531−534.
(7) Velev, O. D.; Jede, T. A.; Lobo, R. F.; Lenhoff, A. M. *Chem. Mater.* **1998**, *10*, 3597−3602.
(8) Jiang, P.; Hwang, K. S.; Mittleman, D. M.; Bertone, J. F.; Colvin, V. L. *J. Am. Chem. Soc.* **1999**, *121*, 11630−11637.
(9) Turner, M. E.; Trentler, T. J.; Colvin, V. L. *Adv. Mater.* **2001**, *13*, 180−183.
(10) Yan, H. W.; Blanford, C. F.; Smyrl, W. H.; Stein, A. *Chem. Commun.* **2000**, 1477−1478.
(11) Yablonovitch, E.; Gmitter, T. J. *Phys. Rev. Lett.* **1989**, *63*, 1950−1953.
(12) Lee, W.; Pruzinsky, S. A.; Braun, P. V. *Adv. Mater.* **2002**, *14*, 271−274.
(13) Jiang, P.; Ostojic, G. N.; Narat, R.; Mittleman, D. M.; Colvin, V. L. *Adv. Mater.* **2001**, *13*, 389−393.
(14) Vlasov, Y. A.; Deutsch, M.; Norris, D. J. *Appl. Phys. Lett.* **2000**, *76*, 1627−1629.
(15) Pan, G. S.; Kesavamoorthy, R.; Asher, S. A. *J. Am. Chem. Soc.* **1998**, *120*, 6525−6530.
(16) Vos, W. L.; Sprik, R.; vanBlaaderen, A.; Imhof, A.; Lagendijk, A.; Wegdam, G. H. *Phys. Rev. B: Condens. Matter* **1996**, *53*, 16231−16235.
(17) Lee, K.; Asher, S. A. *J. Am. Chem. Soc.* **2000**, *122*, 9534−9537.
(18) Chutinan, A.; Noda, S. *Phys. Rev. B: Condens. Matter* **2000**, *62*, 4488−4492.
(19) Pan, G. S.; Kesavamoorthy, R.; Asher, S. A. *Phys. Rev. Lett.* **1997**, *78*, 3860−3863.
(20) Mach, P.; Wiltzius, P.; Megens, M.; Weitz, D. A.; Lin, K.-h.; Lubensky, T. C.; Yodh, A. G. *Phys. Rev. E* **2002**, *65*, 031720/031721−031720/031723.
(21) Vlasov, Y. A.; Yao, N.; Norris, D. J. *Adv. Mater.* **1999**, *11*, 165−169.
(22) Lyon, L. A.; Kong, S. B.; Eustis, S.; Debord, J. D. *Polym. Prepr.* **2002**, *43*, 24−25.
(23) Joannopoulos, J. D.; Meade, R. D.; Winn, J. N. *Photonic Crystals: Molding the Flow of Light*; Princeton University Press: Princeton, 1995.

is difficult to imagine the utilization of standard colloidal self-assembly methods to precisely and accurately introduce defects into a structure. In this regard, photolithographic techniques have a distinct advantage over self-assembly methods, as the photonic/defect structure can be determined in the process design phase, with subsequent translation to the material being accomplished in a directed and perhaps automated fashion. In light of the limitations of self-assembly methods and the advantages of optical patterning, others have created patterned crystals by combining colloidal assembly with spatially directed methods such as multiphoton photopolymerization.[12]

The work presented herein similarly describes the photodirected creation of defects in colloidal crystals, albeit at a much longer length scale. While the methods presented here will not immediately result in photonic guiding structures due to their low refractive index contrast and the relatively large size of the defect structures, they may lead to more technologically relevant assemblies in the future. In this approach, colloidal hydrogel particles composed of the thermoresponsive polymer poly-*N*-isopropylacrylamide (pNIPAm) are used to assemble colloidal crystals that can be reversibly interconverted between a glassy, disordered state and a crystalline state by cycling the temperature across the characteristic volume phase transition temperature (VPTT) of the particles (∼32 °C).[26,27] These pNIPAm particles are lightly cross-linked (∼5 mol % *N,N*′-methylene(bisacrylamide)) network polymers that contain >90% water by volume in their swollen state. At the VPTT, the particles deswell via an entropically favored phase separation event in which the vast majority of the water is expelled from the network.[28,29] This transition manifests itself as a large particle size change. Co-assembly of hydrogel particles with Au nanoparticles affords a material that undergoes the crystal/glass transition when addressed with light of a wavelength that is resonant with the Au nanoparticle plasmon absorption. The Au particles absorb the incident radiation and then relax by nonradiative processes, thereby heating the surrounding material.[30−32] By modulation of the incident laser power and/or Au doping level, one can then modulate the local temperature in the hydrogel assembly and thereby control formation of glassy materials from colloidal crystals or anneal crystalline regions into glassy structures. This approach may offer a new route to the patterning of photonic structures from self-assembled precursor materials.

Experimental Section

Materials. All reagents were purchased from Sigma-Aldrich unless noted otherwise. *N*-Isopropylacrylamide (NIPAm) was recrystallized from hexanes (J. T. Baker) and dried in vacuo prior to use. *N,N*′-Methylenebisacrylamide (BIS), sodium dodecyl sulfate (SDS), ammonium persulfate (APS), hydrogen tetrachloroaurate(III) trihydrate, and trisodium citrate dihydrate were all used as received. Water for all reactions, solution preparation, and polymer purification was first

distilled then deionized to a resistance of 18 MΩ (Barnstead E-Pure system) and finally filtered through a 0.2 μm filter to remove particulate matter.

Polymerization. Microgels were prepared via aqueous free-radical precipitation polymerization in a manner similar to that previously reported.[33] Polymerization was performed in a three-neck, 200 mL round-bottom flask equipped with a magnetic stir-bar, reflux condenser, thermometer, and nitrogen inlet. All monomers (70 mM total concentration, NIPAm:BIS 95:5) and surfactant (1 mM) were dissolved in 100 mL of H$_2$O and then filtered through a 0.2 μm membrane filter (Pall Gelman Metricel) to remove any remnant particulate matter. Under a stream of nitrogen and with constant stirring, the solution was heated to 70 °C and allowed to thermally stabilize for a period of at least 1 h. Next, free-radical polymerization was initiated with APS (0.26 mmol) dissolved in 1 mL of heated (70 °C) H$_2$O; the stirring solution was allowed to react for a period of 5 h under nitrogen. All particles used for assembly of colloidal crystals were purified via dialysis (Spectra/Por 7 dialysis membrane, MWCO 10 000, VWR) against daily changes of H$_2$O for 2 weeks at 5 °C.

Colloidal Au Synthesis. Colloidal Au was prepared according to methods previously reported.[34] Briefly, a 250 mL stirring solution of 1.0 mM HAuCl$_4$ was heated to a vigorous boil. A 25 mL solution of 38.8 mM sodium citrate was then added rapidly to produce a pale-yellow solution that quickly changed color to a deep burgundy. Boiling was continued for 10 min following the color change, after which the heating source was removed and stirring was allowed to proceed for 15 min. Transmission electron microscopy (TEM, JEOL 1210 Analytical TEM) analysis indicated a particle diameter of 16 ± 1.6 nm.

Photon Correlation Spectroscopy. Hydrogel particle sizes and polydispersities were determined via photon correlation spectroscopy (PCS, Protein Solutions Inc.) as previously reported.[26] Microgels were analyzed in a three-sided quartz cuvette into which was placed 0.5 mL of a 10 μg/mL particle solution. The sample was allowed to equilibrate at the proper temperature for 5 min before data collection. Scattered light was collected at 90° by a single-mode optical fiber coupled to an avalanche photodiode detector. Data were analyzed with Protein Solutions' Dynamics Software Version 5.25.44.

Crystal Assembly. A 1.5 mL solution containing various ratios of microgel:colloidal Au was placed into a centrifuge tube and centrifuged at 26 °C, at a relative centrifugal force of 16 100*g* for 75 min; the clear, colorless supernatant solution was removed following centrifugation. Colloidal Au was redispersed throughout the microgel pellet by repeated heating (35 °C), agitating, and sonicating. The sample was then heated to 35 °C and injected into a cell with a total volume of 0.057 mL consisting of an oval 19 × 6 × 0.5 mm perfusion gasket (Molecular Probes) sandwiched between two microscope cover glasses (22 × 22 mm, Fisher). The sample cell was heated to 50 °C and held for 10 min, after which the sample was cooled to room temperature at a rate of approximately 0.2 °C/min to obtain bulk crystallization. Transmission spectra were collected on a Shimadzu UV-1601 spectrophotometer.

Microscopy. All microspectrophotometric measurements and imaging were performed on an Olympus IX-70 inverted microscope using a low numerical aperture 10X objective (N.A. = 0.25).[27] Images were aquired with a Photometrics CoolSNAP color CCD and processed with CoolSNAP software v1.2. For microspectrophotometric analysis, reflected white light (Olympus U-ULH tungsten halogen source) from the sample was imaged through a monochromator (ISA Triax 320, grating = 600 grooves/mm, slit width = 0.5 mm) onto a black and white CCD camera (Javelin, JE-7442). Spectral images (sample position vs wavelength) were collected with a framegrabber, and intensity profiles were processed with Scion Image Beta v4.0.2 software. Similar experimental approaches to the measurement of single-domain optical

(24) Lin, S.-Y.; Chow, E.; Hietala, V.; Villeneuve, P. R.; Joannopoulos, J. D. *Science* **1998**, *282*, 274−276.
(25) Joannopoulos, J. D.; Villeneuve, P. R.; Fan, S. *Nature* **1997**, *387*, 830.
(26) Debord, J. D.; Lyon, L. A. *J. Phys. Chem. B* **2000**, *104*, 6327−6331.
(27) Debord, J. D.; Eustis, S.; Debord, S. B.; Lofye, M. T.; Lyon, L. A. *Adv. Mater.* **2002**, *14*, 658−661.
(28) Pelton, R. *Adv. Colloid Interface Sci.* **2000**, *85*, 1−33.
(29) Saunders, B. R.; Vincent, B. *Adv. Colloid Interface Sci.* **1999**, *80*, 1−25.
(30) Link, S.; El-Sayed, M. A. *Int. Rev. Phys. Chem.* **2000**, *19*, 409−453.
(31) Sershen, S. R.; Westcott, S. L.; Halas, N. J.; West, J. L. *J. Biomed. Mater. Res.* **2000**, *51*, 293−298.
(32) Sershen, S. R.; Westcott, S. L.; West, J. L.; Halas, N. J. *Appl. Phys. B* **2001**, *73*, 379−381.

(33) Jones, C. D.; Lyon, L. A. *Macromolecules* **2000**, *33*, 8301−8306.
(34) Grabar, K. C.; Freeman, R. G.; Hommer, M. B.; Natan, M. J. *Anal. Chem.* **1995**, *67*, 735−743.

properties have been presented previously.[14] The method works by placing the entrance slit of the monochromator in the image plane of the side (ccd) port of the microscope. The slit width and height then determine the portion of the image that is passed through the monochromator. Thus, a very narrow horizontal slice of the image is spectrally dispersed and then imaged on a ccd camera placed at the monochromator exit port. The obtained image then has a spatial vertical axis and a horizontal wavelength axis. Horizontal line scans of the image thereby represent reflectance spectra of a specific region of the image. Of particular importance to this technique is the ability to obtain spectra from specific areas of the sample (e.g., single crystals or single domains), so as to remove inhomogeneous line broadening effects that may be present in polycrystalline samples. By performing simultaneous imaging and spectroscopic analysis, we found that the obtained spectra can be directly correlated to a spatial position on the sample. Furthermore, the position-to-position variability in spectral properties can be determined by this method.[14,27]

Photothermal Crystallization and Melting. The following were used as laser sources: a 532 nm pulsed Nd:YAG (Uniphase) and a 632.8 nm CW HeNe (Spectra-Physics). Photothermal crystallization was performed by placing a sample cell consisting of a glassy-phase material 15 cm from the Nd:YAG laser souce. The sample was irradiated for 5 min (0.87 W/cm^{2}) to produce crystallization in the area of the beam. Photothermal melting was performed by placing a thermally annealed crystalline sample 5 cm from the laser source (where the power increases to 3.4 W/cm^{2} due to the smaller diameter of the beam) while irradiating for 22 s.

Results and Discussion

As described in previous publications, the formation of pNIPAm hydrogel colloidal crystals proceeds from a kinetically trapped amorphous or glassy phase to a thermodynamically preferred close-packed crystalline phase via a thermal annealing step.[26,27] The amorphous state is described as such due to the lack of a Bragg peak and the lack of obvious color in the sample. In the vernacular of condensed matter physics, such a state is often referred to as "glassy" because the hard sphere analogue is a solid without any long-range order. However, the microgel systems investigated here are more appropriately described as amorphous, viscous fluids, because they are not truly solid in structure. For brevity, we will refer to the amorphous state as glassy, because it is likely that the microgel photonic crystals described here are structurally similar to their hard sphere cousins. The term is not, however, meant to convey the concept of a hard solid.

In the annealing step, the noncrystalline material obtained from centrifugal concentration of the particles is raised above the VPTT temperature of pNIPAm and then cooled back to room temperature. This process can be monitored by observing the optical properties of the assembly as shown in Figure 1. Prior to the annealing step, the extinction spectrum of a centrifuged sample of ∼224 nm diameter hydrogel particles is broad and featureless, indicative of a lack of long-range particle ordering.

When the sample is raised above the VPTT and then cooled slowly back to room temperature, a Bragg peak evolves as the particles order into a colloidal crystal. While the exact structure of the kinetically trapped glass is unknown, the extreme softness of the particles may contribute to this state by allowing compression and/or deformation of the particles during the centrifugation process. Such a material would resist spontaneous ordering as the translational diffusion coefficient of the tightly packed particles should be very small. By raising the temperature above the volume phase transition, we found that the component
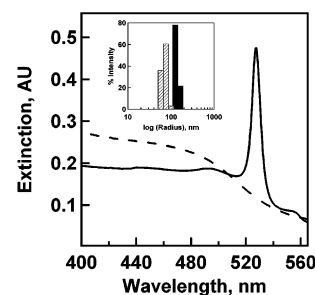

Figure 1. Extinction spectra depicting the spectral properties of representative glassy (- - -) and crystalline (—) assemblies of ∼224 nm diameter pNIPAm particles. The spectrum of the glassy material was obtained following centrifugal concentration of the particles and prior to thermal annealing, while the spectrum of the crystalline material was obtained from the same sample following thermal annealing. Path length = 0.5 mm. Inset: PCS-determined particle size distributions for particles used crystal assembly. The solid bars (larger radius) correspond to the particles at 25 °C, while the smaller particle size was obtained at 40 °C.

hydrogel particles shrink manyfold in volume by expelling water from the network.[28] This deswelling event then increases the particle translational diffusion coefficient by simultaneously decreasing both the particle size and the particle volume fraction in the assembly. In the case of the ∼224 nm diameter particles used here, photon correlation spectroscopy measurements show that the particle diameter above the VPTT is ∼120 nm, which corresponds to a volume decrease of ∼6.5-fold. As the temperature is lowered below the VPTT, the particles reswell, presumably under conditions that favor the formation of a thermodynamically preferred crystal, where the particles order into a periodic lattice, thus producing a strongly diffracting material. Previous studies have shown that the obtained crystalline material is cubic close packed (fcc or rhcp) with the particles being spherical in shape.[27]

Co-assembly of colloidal Au with the colloidal pNIPAm particles is accomplished by simply adding an aqueous colloidal Au suspension (citrate stabilized) to the hydrogel suspension prior to centrifugation. During the subsequent centrifugation step, the two types of particles sediment at different rates, with the smaller, denser colloidal Au separating from the solution faster than the larger but more buoyant hydrogel particles. Under these conditions, the Au particles do not noticeably aggregate and can be easily redispersed into the hydrogel mass (following decantation of the supernatant solvent) by gentle sonication and agitation. This process is illustrated pictorially in Scheme 1.

The optical properties of the resultant materials appear to be a simple convolution of the optical properties of the colloidal Au and the crystal or glass, depending on the annealing history of the sample. Figure 2a shows representative extinction spectra for a series of Au/hydrogel assemblies prior to annealing. In this figure, colloidal Au concentrations in particles/mL are indicated for each spectrum. When no Au is included in the sample, the typical broad extinction associated with the glassy material is evident. As the concentration of Au is increased, the extinction at ∼520 nm increases due to the colloidal Au plasmon absorption. Upon bulk thermal annealing of the samples, the Au plasmon absorption becomes more resolved as the short-wavelength extinction associated with the glassy material decreases, while a sharp Bragg peak associated with the colloidal crystal becomes evident (Figure 2b). These results suggest that the inclusion of colloidal Au in the crystal does

Scheme 1. Assembly Process for Colloidal Au-Doped Microgel Colloidal Crystals
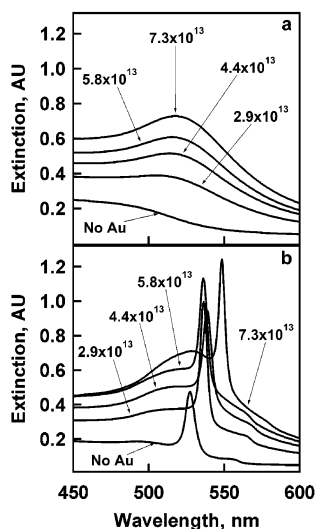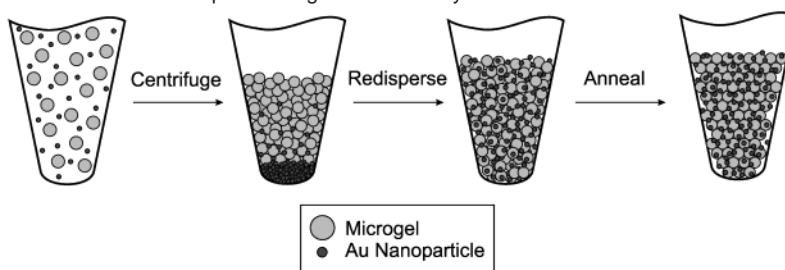
Figure 2. Extinction spectra of colloidal Au-doped microgel assemblies as a function of colloidal Au concentration. Panel a depicts the optical properties of the assemblies prior to thermal annealing, while panel b shows the optical properties of the fully annealed crystalline samples. Colloidal Au concentrations in particles/mL are indicated in the figure legends. Path length = 0.5 mm.

not significantly perturb the crystallization process. The Bragg peaks for crystals containing colloidal Au tend to appear at longer wavelengths than the undoped crystals, suggesting that the particles assemble with a slightly larger lattice constant when in the presence of colloidal Au.

Because the above data illustrate that the bulk glassy-to-crystalline conversion can be induced by radiant heating, it should also be possible to use the colloidal Au to photothermally address the assemblies. This process relies on the large extinction coefficient of Au nanoparticles at the plasmon resonance ($\sim 1 \times 10^9$ M^{-1} cm^{-1} at 520 nm for 20 nm diameter colloidal Au) and the extremely small photoemission quantum yield for such particles.[30] As a result, the energy absorbed upon plasmon excitation is largely re-emitted via nonradiative pathways, thereby heating the bath surrounding the particle. Halas and West have used these effects to photothermally deswell pNIPAm monoliths doped with metal nanoshells.[31,32] In those studies, the relevant plasmon absorption was in the near-IR region of the spectrum allowing for addressability at wavelengths suitable for subdermal drug delivery using CW diode lasers. In the present case, a diode-pumped, frequency doubled Nd:YAG laser ($\lambda = 532$ nm) is used to address the assemblies. This wavelength is slightly longer than the plasmon extinction maximum, but significant absorption still exists at this wavelength. First, we shall address the effect of irradiating a glassy sample at 532 nm; the irradiation geometry is described in detail in the Experimental Section. Figure 3 shows an optical micrograph
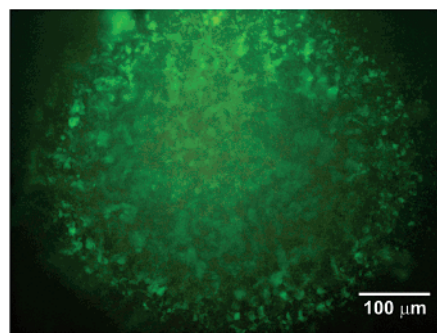
Figure 3. Optical micrograph of a crystalline region that has been photothermally introduced into a glassy sample containing 7.3×10^{13} Au particles/mL after 5 min of illumination.
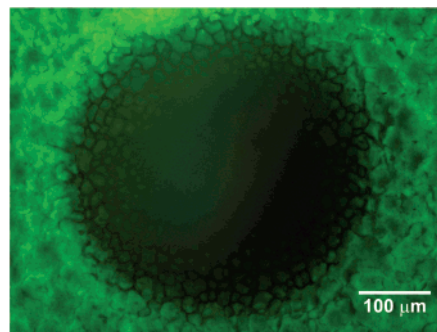
Figure 4. Optical micrograph of a glassy region photothermally introduced into a crystalline sample containing 7.3×10^{13} Au particles/mL after 22 s of illumination at 3.4 W/cm^2.

of the illuminated region of a glassy material containing 7.3×10^{13} Au particles/mL after 5 min of irradiation with a 0.95 mm diameter beam (incident power = 0.87 W/cm^2). An $\sim$0.55 mm diameter circular region of brightly reflective polycrystalline material is observable, surrounded by a faintly colored glassy region. In contrast, samples that did not contain colloidal Au did not show any morphological changes upon illumination. The crystallization process actually begins within 30 s of irradiation as indicated by microscopy. Regions created within this time frame are ill-defined but do show spectral properties similar to those of the feature shown in Figure 4. These data are interpreted as being the result of photothermal heating, with the Au nanoparticles being the sensitizing moieties. Irradiation of the plasmon mode results in local heating around the Au particles, thereby causing partial deswelling of the hydrogel particles. These particles are then able to diffuse more readily than in their swollen state, thus allowing for crystal nucleation and growth within the laser spot. Apparently, these irradiation conditions lead to a local temperature increase that is appropriate for annealing the assembly to the crystalline state from the glassy state.
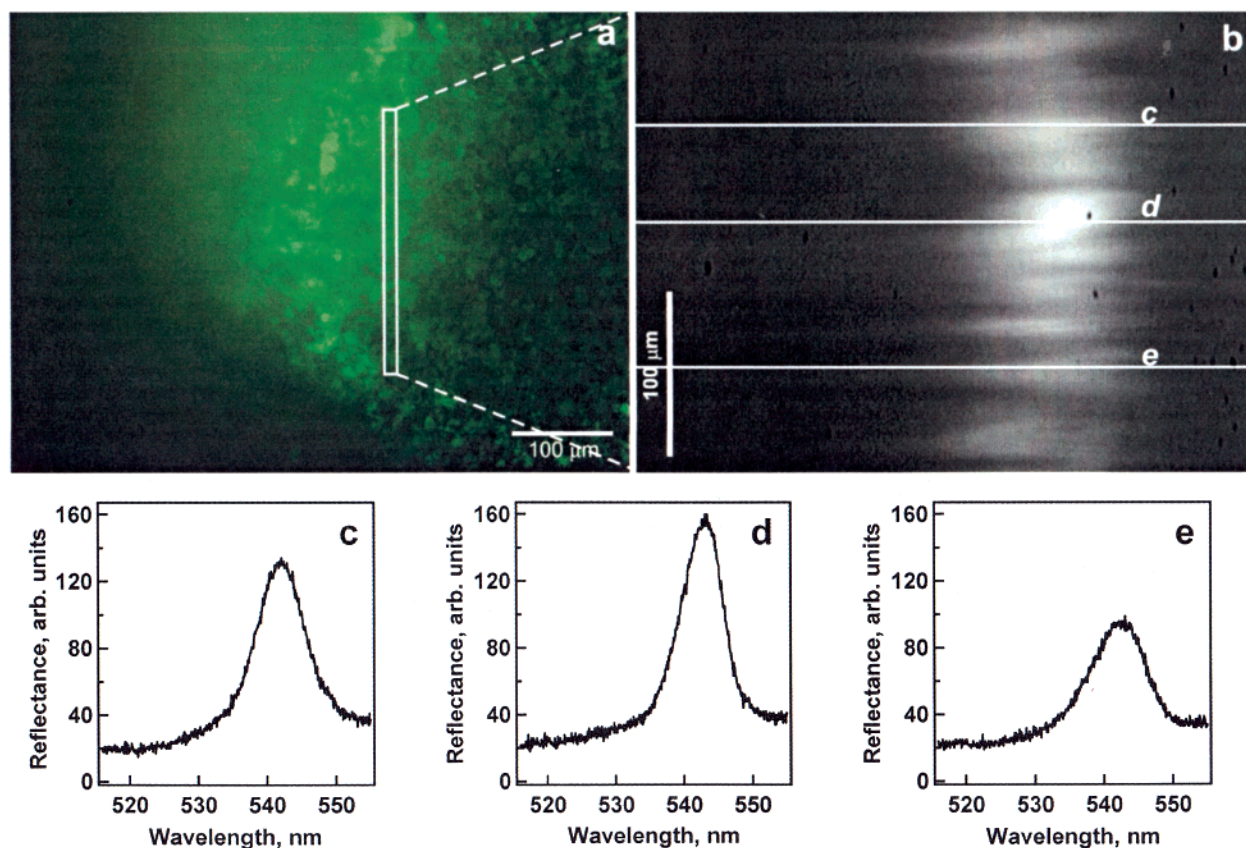
Figure 5. (a) Optical micrograph of both glassy and crystalline phases following photothermal excitation of a glassy sample. This image was acquired from a slightly different portion of the same sample shown in Figure 3 so as to clearly show both phases. (b) Spectral image acquired from the indicated region of the real-space image. Bright spots in the image indicate high reflectivity and hence indicate the position and breadth of the Bragg peaks. (c–e) Line profiles taken from the indicated spots on the spectral image shown in (b).

While excitation of the Au particles under certain conditions yields glass-to-crystal transitions, irradiation of precrystallized materials under higher power conditions allows for conversion of the crystalline material to a glassy one. The results of this process are shown in Figure 4, where now a circular glassy region is formed inside a brightly reflective crystalline sample after only 22 s of laser irradiation at 3.4 W/cm^2. This sample is the same one used to produce the image shown in Figure 3. Here, the sample was precrystallized by the thermal method described in the Experimental Section. In this case, it is proposed that the assembled crystal is photothermally excited to a temperature above the melting point, where again the particles deswell and begin to diffuse freely.

Microspectrophotometric interrogation of each region of the feature shown in Figure 3 clearly shows the dramatic differences in optical properties. Figure 5b is the spectral image acquired from the indicated region of the real-space image (Figure 5a). The *y*-axis of this image corresponds to the spatial dimension, while the *x*-axis corresponds to wavelength. As such, the optical properties of a large portion of the crystalline region can be correlated directly with the image. Figure 5c–e shows representative line-scans taken from different regions of the spectral image, thus illustrating the relative spectral homogeneity of the crystalline region. The data suggest relatively homogeneous crystal orientations and lattice constants. Conversely, the spectral image acquired from a glassy region in Figure 4 shows no structure resulting from Bragg diffraction in the assembly (see Supporting Information).

The above results illustrate our ability to interconvert glassy and crystalline phases in colloidal Au-doped hydrogel assemblies using laser irradiation. However, they do not definitively address the origin of these effects. It has been assumed that photothermal annealing results from plasmon excitation of the Au nanoparticles. To define more clearly the nature of the excitation beam that is required to achieve these results, a HeNe laser ($\lambda = 632.8$ nm) was used to address the sample at a wavelength longer than the plasmon band. Interestingly, this laser also induced a small degree of crystallization in a glassy sample after ~2 h of illumination (4.1 W/cm^2). It is apparent that the longer wavelength excitation is able to induce some local heating, albeit with much longer irradiation times and much higher power, perhaps through some remnant absorption of the Au nanoparticles at that wavelength. Recall that the samples shown in Figures 3–5 were prepared in less than 15 min using a Nd: YAG laser operating at a power of 0.87 or 3.4 W/cm^2, thus suggesting that the annealing/melting process is indeed wavelength dependent.

Conclusions

We have demonstrated the co-assembly of pNIPAm hydrogel particles and nanosized colloidal Au into colloidal crystals by a centrifugation/thermal annealing method. The resultant assemblies can then be further manipulated by illumination with light that is resonant with the colloidal Au plasmon absorption. This absorption process is accompanied by a subsequent local heating of the surrounding hydrogel material, which then

undergoes a thermally initiated deswelling event. The deswollen particles are then allowed to either assemble into a crystalline phase or disorder into a glassy phase, depending on the illumination time, laser power, and the initial state (crystalline vs glassy) of the assembly. This effect is wavelength dependent, with the heating effect being much less efficient if the incident radiation is not resonant with the colloidal Au plasmon band.

Supporting Information Available: Real-space and spectral images of photopatterned crystalline and glassy regions, along with representative line-scan spectra (PDF). This material is available free of charge via the Internet at http://pubs.acs.org.

JA027431X